
Comparison of 3 Interpretation Criteria for ^{68}Ga -PSMA11 PET Based on Inter- and Intrareader Agreement

Akira Toriihara*, Tomomi Nobashi*, Lucia Baratto, Heying Duan, Farshad Moradi, Sonya Park, Negin Hatami, Carina Mari Aparici, Guido Davidzon, and Andrei Iagaru

Division of Nuclear Medicine and Molecular Imaging, Department of Radiology, Stanford University, Stanford, California

PET using radiolabeled prostate-specific membrane antigen (PSMA) is now being more widely adopted as a valuable tool to evaluate patients with prostate cancer (PC). Recently, 3 different criteria for interpretation of PSMA PET were published: the European Association of Nuclear Medicine (EANM) criteria, the Prostate Cancer Molecular Imaging Standardized Evaluation criteria, and the PSMA Reporting and Data System. We compared these 3 criteria in terms of interreader, intrareader, and intercriteria agreement. **Methods:** Data from 104 patients prospectively enrolled in research protocols at our institution were retrospectively reviewed. The cohort consisted of 2 groups: 47 patients (mean age, 64.2 y old) who underwent Glu-NH-CO-NH-Lys-(Ahx)-[^{68}Ga (HBED-CC)] (^{68}Ga -PSMA11) PET/MRI for initial staging of biopsy-proven intermediate- or high-risk PC, and 57 patients (mean age, 70.5 y old) who underwent ^{68}Ga -PSMA11 PET/CT because of biochemically recurrent PC. Three nuclear medicine physicians independently evaluated all ^{68}Ga -PSMA11 PET/MRI and PET/CT studies according to the 3 interpretation criteria. Two of them reevaluated all studies 6 mo later in the same manner and masked to the initial reading. The Gwet agreement coefficient was calculated to evaluate interreader, intrareader, and intercriteria agreement based on the following sites: local lesion (primary tumor or prostate bed after radical prostatectomy), lymph node metastases, and other metastases. **Results:** In the PET/MRI group, interreader, intrareader, and intercriteria agreement ranged from substantial to almost perfect for any site according to all 3 criteria. In the PET/CT group, interreader agreement ranged from substantial to almost perfect except for judgment of distant metastases based on the PSMA Reporting and Data System (Gwet agreement coefficient, 0.57; moderate agreement), in which the most frequent cause of disagreement was lung nodules. Intrareader agreement ranged from substantial to almost perfect for any site according to all 3 criteria. Intercriteria agreement for each site was also substantial to almost perfect. **Conclusion:** Although the 3 published criteria have good interreader and intrareader reproducibility in evaluating ^{68}Ga -PSMA11 PET, there are some factors causing interreader disagreement. Further work is needed to address this issue.

Key Words: ^{68}Ga -PSMA11; PET/CT; PET/MRI; interpretation criteria; interreader agreement

J Nucl Med 2020; 61:533–539
DOI: 10.2967/jnumed.119.232504

Received Jun. 14, 2019; revision accepted Aug. 27, 2019.
For correspondence or reprints contact: Andrei Iagaru, Division of Nuclear Medicine and Molecular Imaging, Department of Radiology, Stanford University, 300 Pasteur Dr., Stanford, CA 94305.
E-mail: aiagaru@stanford.edu
*Contributed equally to this work.
Published online Sep. 27, 2019.
COPYRIGHT © 2020 by the Society of Nuclear Medicine and Molecular Imaging.

Prostate cancer (PC) is the most common malignancy occurring in men in the United States and Europe (1,2). Radiopharmaceuticals targeting prostate-specific membrane antigen (PSMA) can be used for both imaging and treatment in many patients with PC (3). The use of Glu-NH-CO-NH-Lys-(Ahx)-[^{68}Ga (HBED-CC)] (^{68}Ga -PSMA11) PET is rapidly expanding both at initial staging and for evaluation of biochemical recurrence (BCR) of PC. The usefulness of ^{68}Ga -PSMA11 PET/MRI for detection and initial staging of PC has also been reported (4,5). ^{68}Ga -PSMA11 PET/CT has excellent accuracy in detecting BCR PC (pooled per-patient sensitivity and specificity of 80% and 97%, respectively) (6). ^{68}Ga -PSMA11 PET/CT can often change the treatment strategy at BCR (range, 28.6%–87.1%) (7).

^{68}Ga -PSMA11 PET/MRI and PET/CT have great potential to improve management of patients with PC. However, to make the most of these modalities, appropriate image interpretation is needed in terms of not only accuracy but also reproducibility among readers. A previous study showed good interobserver agreement in evaluating ^{68}Ga -PSMA11 PET/CT (8). Three different criteria were published to improve objectivity and accuracy in image interpretation for PSMA PET: the European Association of Nuclear Medicine (EANM) criteria (9), the Prostate Cancer Molecular Imaging Standardized Evaluation (PROMISE) criteria (10), and the PSMA Reporting and Data System (PSMA-RADS) (11). Table 1 summarizes the differences among these criteria.

Here, we compared the 3 PSMA PET interpretation criteria in terms of interreader, intrareader, and intercriteria agreement.

MATERIALS AND METHODS

Patients

Data from 104 patients prospectively enrolled in research protocols at our institution were retrospectively reviewed. The protocols were approved by the local institutional review board (Stanford University Research Compliance Office). Written informed consent was obtained from every participant. The cohort consisted of 2 groups. The first group included 47 patients (mean age, 64.2 ± 6.1 y) who underwent ^{68}Ga -PSMA11 PET/MRI for initial staging. The second group included 57 patients (mean age, 70.5 ± 6.7 y) who underwent ^{68}Ga -PSMA11 PET/CT for BCR PC. Patient characteristics for both groups are shown in Table 2.

^{68}Ga -PSMA11 PET/MRI Protocol

^{68}Ga -PSMA11 was synthesized according to previous reports (12). No specific patient preparation was required. The administered ^{68}Ga -PSMA-11 dose was 91.4–236.4 MBq (mean \pm SD, 155.4 ± 30.7 MBq). After 41–69 min (mean, 49.9 ± 5.3 min) from injection, whole-body scanning from vertex to mid thighs was performed using a Signa PET/MR scanner (GE Healthcare). Detailed imaging protocols were shown in a previous publication (5). Briefly, PET data from vertex

TABLE 1
Comparison Among 3 Interpretation Criteria for ⁶⁸Ga-PSMA PET

Parameter	EANM (9)	PROMISE (10)	PSMA-RADS (11)
Summary	All areas of increased PSMA uptake in sites not expected to show physiologic uptake are to be reported as “anomalous,” followed by subclassification to 3 categories	Both CT/MRI appearance and PSMA uptake are considered, and diagnosis is judged as “positive,” “equivocal,” or “negative” for each site	All abnormal findings are classified by 5-point scale based on possibility of cancerous lesion
Definition of significant uptake	Focal uptake higher than adjacent background	Basically, uptake equal to or above liver	Not clearly defined
Lesion site	Local sites, local lymph nodes, distant lymph nodes, skeletal, other	Local sites before and after treatment, lymph nodes, bone/visceral organ	Bone, soft tissue (including lymph nodes)
Classification in each site	Anomalous, pathologic, uncertain, nonpathologic, normal	Positive, equivocal, negative	5: PC almost certainly present; 4: PC highly likely; 3: equivocal (3A–D); 2: likely benign; 1: benign (1A/B)
Final judgment	Abnormal (pathologic), normal	Positive, equivocal, or negative, plus miTNM classification	Highest PSMA-RADS score among detected lesions

miTNM = molecular imaging TNM.

to mid thighs were acquired in 3-dimensional (3D) mode and for 4 min per bed position, followed by image reconstruction with ordered-subsets expectation maximization (2 iterations and 28 subsets). As MRI sequences, axial 2-point Dixon 3D T1-weighted spoiled gradient-echo images, coronal T2-weighted single-shot fast spin echo images, and coronal diffusion-weighted images were obtained. The Dixon sequence and PET data were acquired at the same table position and time so as to ensure optimal temporal and regional correspondence on fused PET/MR images. Dedicated pelvic PET/MRI was subsequently acquired; however, these PET data were not used in the analysis to match the whole-body acquisition from PET/CT.

⁶⁸Ga-PSMA11 PET/CT Protocol

The administered ⁶⁸Ga-PSMA-11 dose was 111–199.8 MBq (mean, 145.8 ± 14.8 MBq). After 44–90 min (mean, 61.4 ± 13.6 min) from injection, whole-body scans from vertex to mid thighs were performed using a Discovery 690 (*n* = 18) or Discovery MI (*n* = 39) PET/CT scanner (GE Healthcare). The parameters for unenhanced CT for attenuation correction and anatomic localization were as follows:

10 mA, 120 kV, 512 × 512 matrix, and 867-mm field of view, in 22.5 s. PET data were acquired in 3D mode with a matrix of 256 × 256 for 3 min per bed position. The PET images were reconstructed using ordered-subsets expectation maximization with 2 iterations and 24 subsets for the Discovery 690 scanner and with 3 iterations and 16 subsets for the Discovery MI scanner.

Interpretation of ⁶⁸Ga-PSMA11 PET/MRI and PET/CT Studies

Images were interpreted by 3 nuclear medicine physicians (with 14, 11, and 8 y of experience). They separately evaluated all PET/MRI and PET/CT datasets using each set of criteria. The readers were masked to all clinical information other than the indication for the scan as initial staging or BCR. To determine the category in the RADS for prostate imaging (PI-RADS) (13) for evaluating primary tumors based on PROMISE criteria, contrast-enhanced multiparametric prostate MRI within 3 mo of PET/MRI was referenced. In 17 patients (36.2%) whose prior prostate MRI results were unavailable, the category was determined on the basis of the diagnostic MR component

TABLE 2
Patients' Characteristics

Characteristic	PET/MRI for initial staging	PET/CT due to BCR
<i>n</i>	47	57
Age (y)	64.2 ± 6.1 (44–74)	70.5 ± 6.7 (58–89)
Prostate-specific antigen (ng/mL)	10.4 ± 8.4 (3.3–50.4)	35.7 ± 172.2 (0.2–1.170)
Injected dose (MBq)	155.4 ± 30.7 (91.4–236.4)	145.8 ± 14.8 (111–199.8)
Uptake time (min)	49.9 ± 5.3 (41–69)	61.4 ± 13.6 (44–90)
Treatment before PET/CT	Not applicable	Prostatectomy, 41; radiotherapy, 32; brachytherapy, 6; hormonal therapy, 36; chemotherapy, 3; ²²³ Ra, 1

Continuous data are expressed as mean ± SD, followed by range in parentheses.

TABLE 3
Definition of Each Judgment

Parameter	Reference*	EANM	PROMISE	PSMA-RADS
Each lesion site	Positive	Pathologic	Positive	PSMA-RADS-4/5
	Equivocal	Uncertain	Equivocal	PSMA-RADS-3
	Negative	Nonpathologic/normal	Negative	PSMA-RADS-1/2
Final judgment per patient	Positive	Abnormal	Positive	PSMA-RADS-4/5
	Equivocal	Not applicable	Equivocal	PSMA-RADS-3
	Negative	Normal	Negative	PSMA-RADS-1/2

*These judgments were used for statistical analyses in this study.

from the PET/MRI study. One of the readers referred to clinical interpretation reports or the PI-RADS score determined by a radiologist (with 5 y of experience in prostate MRI). Finally, judgments by all 3 readers were used for evaluating interreader agreement.

Six months later, 2 physicians performed the second evaluation of all PET/MRI and PET/CT studies in the same manner. These second judgments were used to evaluate intrareader agreement for each site and set of criteria. These judgments were also used to evaluate intercriteria agreement. When judgments by the 2 readers matched, they could be directly applied for the following analyses. When judgments did not match, another nuclear medicine physician (with 12 y of experience) evaluated each study and chose the judgment that she regarded as more appropriate.

Statistical Analysis

We defined 3 categories (positive, equivocal, and negative) as references for each judgment to apply to the statistical analysis (Table 3). For local sites, lymph node metastases, distant metastases, and the final judgment per patient, the Gwet agreement coefficient (AC) (14) was calculated to evaluate interreader and intrareader agreement on each set of criteria, as well as intercriteria agreement. The degree of agreement according to the Gwet AC is as follows (15): 0.81–1.00, almost perfect agreement; 0.61–0.80, substantial agreement; 0.41–0.60, moderate agreement; 0.21–0.40, fair agreement; and 0.00–0.20, slight agreement. Stata software (version 15.1; Stata Corp.) was used in these analyses.

RESULTS

Interreader, intrareader, and intercriteria agreement for each site and set of criteria are shown in Tables 4, 5, and 6, respectively.

In the PET/MRI group, interreader agreement ranged from substantial to almost perfect for any site according to all 3 criteria. With the EANM criteria, moderate intensity or diffuse uptake in the prostate led to interreader disagreement in some cases (Fig. 1). Similar to the PET/CT group, there were some cases of interreader disagreement in the evaluation of distant metastases using PSMA-RADS. Thyroid mass (2 patients) (Fig. 2), right renal mass (1 patient), and asymmetric sublingual gland uptake (1 patient) were pointed out by 1 reader, followed by interreader disagreement (equivocal vs. negative). Another patient was judged as positive and equivocal for a first and second sternal lesion, respectively.

In the PET/CT group, interreader agreement was substantial to almost perfect for any site according to all 3 criteria, except in the evaluation of distant metastases based on PSMA-RADS (Gwet AC, 0.57; moderate agreement). The most frequent causes of interreader disagreement in judgments on distant metastases were lung nodules (11 patients) (Fig. 3), followed by bone lesions (7 patients), asymmetric sublingual gland uptake (3 patients) (Fig. 4), pancreatic uptake (1 patient), and masslike thyroid uptake (1 patient).

Interreader agreement on the final judgment may have been influenced by lesion location. The EANM criteria, which lack the “equivocal” category, showed higher Gwet AC than did PROMISE and PSMA-RADS in both the PET/MRI and the PET/CT groups (Table 4).

Intrareader agreement ranged from substantial to almost perfect for any site according to all 3 criteria (Table 5). Intercriteria agreement for each site ranged from substantial to almost perfect (Table 6). However, PSMA-RADS showed a different judgment

TABLE 4
Interreader Agreement for Each Set of Interpretation Criteria (Gwet AC)

Group	Site	EANM	PROMISE	PSMA-RADS
PET/MRI for initial staging	Local sites	0.70	0.75	0.73
	Lymph node metastases	0.93	0.93	0.93
	Distant metastases	0.96	0.97	0.89
	Final judgment	0.89	0.79	0.72
PET/CT due to BCR	Local sites	0.69	0.73	0.77
	Lymph node metastases	0.80	0.79	0.78
	Distant metastases	0.84	0.80	0.57*
	Final judgment	0.79	0.67	0.64

*Moderate agreement.

TABLE 5
Intrareader Agreement for Each Set of Interpretation Criteria (Gwet AC)

Group	Site	EANM	PROMISE	PSMA-RADS
PET/MRI for initial staging	Local sites	0.95/0.63	0.93/0.74	0.98/0.70
	Lymph node metastases	0.93/0.98	0.79/0.98	0.93/0.98
	Distant metastases	0.93/1.00	0.96/0.98	0.98/0.98
	Final judgment	0.95/0.94	0.91/0.77	0.88/0.75
PET/CT due to BCR	Local sites	0.93/0.78	0.91/0.78	0.93/0.78
	Lymph node metastases	0.90/0.79	0.86/0.73	0.86/0.69
	Distant metastases	0.92/0.83	0.83/0.81	0.75/0.81
	Final judgment	0.91/0.73	0.93/0.52*	0.91/0.49*

*Moderate agreement.

Each Gwet AC is expressed as reader 1/reader 2.

(equivocal) from the other criteria (negative) in the evaluation of distant metastasis in 11 and 2 patients of the PET/CT and PET/MRI groups, respectively (Figs. 2 and 3). On the other hand, 2 patients in the PET/MRI group showed complete disagreement among the 3 criteria in the evaluation of local sites with suspected PSMA-ligand–negative PC (Fig. 5).

DISCUSSION

This study shows that the 3 published criteria for evaluating PSMA PET (EANM, PROMISE, and PSMA-RADS) have substantial to almost perfect interreader, intrareader, and intercriteria agreement in most situations. However, throughout this study, we found instances that can lead to disagreement among readers or criteria.

Interreader disagreement most frequently occurred in the evaluation for distant metastases using PSMA-RADS. Particularly, lung nodules appear to lead not only to interreader but also intercriteria disagreement (equivocal vs. negative) in the PET/CT group. Although lung metastases from PC are relatively rare (16,17), small lung nodules can often be problematic in interpretation. Compared with PSMA-RADS, EANM and PROMISE criteria have a greater emphasis on the existence of PSMA uptake. That is, EANM and PROMISE criteria generally regard lesions without elevated PSMA uptake as negative findings (9,10), whereas PSMA-RADS can include such lesions in the equivocal criteria (PSMA-RADS-3D) (11). When

applying these criteria, one should keep in mind that small lesions such as lung nodules can be falsely judged as negative because of the partial-volume effect (17). However, this problem can be solved by clearly stating information on PSMA-negative lesions in the interpretation report, regardless of the criteria used. Similarly, PSMA uptake suggestive of other malignancies also has to be clearly stated in the report, regardless of the criteria used (9–11).

Another consideration regarding interreader disagreement relates to judging disease in the prostate on PSMA PET/MRI or PET/CT. Such disagreement may be due to a difference in interpretation of the definition of “moderate” or “diffuse” uptake (9) according to the EANM criteria among the readers. When the PROMISE criteria are applied, discrepancy in the PI-RADS class may have some effect on interreader disagreement, particularly in a primary tumor with ⁶⁸Ga-PSMA11 uptake less than the liver (10). However, the goal of this work was not to evaluate the PI-RADS criteria, as these have been studied extensively. The use of SUV may improve interreader agreement in terms of the degree of PSMA uptake, although it is not clear whether for PSMA-ligand PET, SUV_{max}, SUV_{mean}, or SUV_{peak} is the most appropriate parameter or whether SUV normalized to body weight or lean body mass should be applied (10,11,18). Further studies are needed to assess each set of interpretation criteria with semiquantitative analysis.

TABLE 6
Intercriteria Agreement for Each Site

Group	Site	Gwet AC
PET/MRI for initial staging	Local	0.92
	Lymph node	0.97
	Distant	0.96
	Final judgment	0.93
PET/CT due to BCR	Local	0.97
	Lymph node	0.98
	Distant	0.72
	Final judgment	0.91

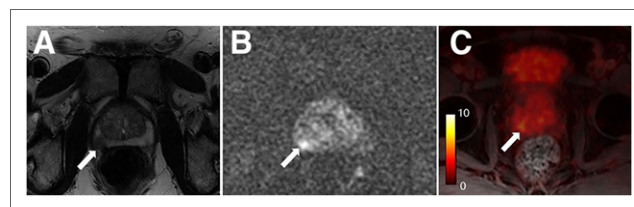


FIGURE 1. A 66-y-old man with biopsy-proven PC (prostate-specific antigen, 5.0 ng/mL; Gleason score, 4 + 4). T2-weighted image (A), diffusion-weighted image (B), and fused PET/MR image (C) are shown. Primary tumor (arrows) in right peripheral zone showed low and high signal intensity on T2-weighted image and diffusion-weighted image, respectively. Although all readers pointed out ⁶⁸Ga-PSMA11 uptake corresponding to this tumor, readers’ judgments based on EANM criteria were discordant (positive vs. equivocal). In such a case, a difference in each reader’s recognition of “focal intense” and “moderate,” referred to in EANM criteria, might lead to interreader disagreement.

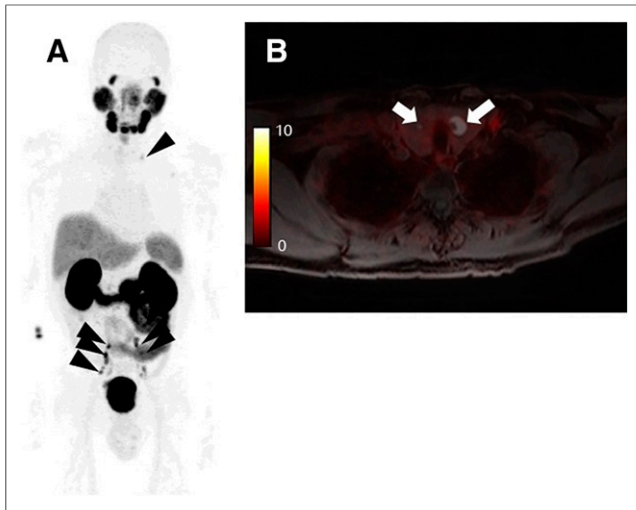


FIGURE 2. A 63-y-old man with biopsy-proven PC (prostate-specific antigen, 50.4 ng/mL; Gleason score, 4 + 5). (A) Maximum-intensity projection image showed multiple lymph node metastases in pelvic and left supraclavicular regions (arrowheads). (B) One reader pointed out thyroid nodules without focal ^{68}Ga -PSMA11 uptake (arrows) and judged them as equivocal (PSMA-RADS-3D), whereas other readers did not refer to these lesions and judged them as negative. Further assessment has not been performed for thyroid.

Our cohort illustrates that physicians interpreting such examinations need to understand physiologic ^{68}Ga -PSMA11 uptake patterns and pitfalls to produce an appropriate evaluation (19,20). ^{68}Ga -PSMA11 is excreted in the urine, and urinary bladder uptake may

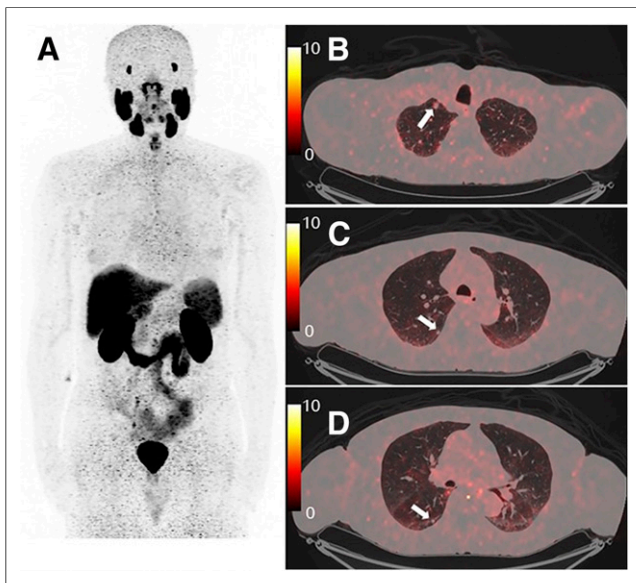


FIGURE 3. A 75-y-old man with BCR PC after radical prostatectomy (prostate-specific antigen, 0.2 ng/mL). (A) Maximum-intensity projection image did not reveal any abnormal ^{68}Ga -PSMA11 uptake. (B–D) However, fused PET/CT images showed multiple lung nodules (arrows). One reader judged these nodules as PSMA-RADS-3D (lesion suggestive of malignancy but lacking uptake), whereas other readers judged them as negative. These nodules were judged as negative by all readers based on EANM and PROMISE criteria because of lack of ^{68}Ga -PSMA11 uptake. Prostate-specific antigen stayed <1.0 ng/mL under bicalutamide treatment.

mask small lesions in patients with BCR or primary tumor in the middle lobe (21,22). Previous studies have proposed adding early- or late-phase PET scans or CT urography to discriminate physiologic ^{68}Ga -PSMA11 uptake in the urinary tract (23–25). ^{68}Ga -PSMA PET11 often shows nonspecific uptake in sympathetic chain, cervical, celiac, and sacral ganglia that can lead to false-positive findings (20,26,27). A typical anatomic localization and ^{68}Ga -PSMA11 uptake pattern can be used to differentiate this nonpathologic uptake from nodal metastases. It is known that other malignant tumors or benign etiologies can also have elevated ^{68}Ga -PSMA11 uptake (18,28–32).

Intrareader agreement was relatively good for each site and for each set of criteria in our study. These results suggest that training for evaluating ^{68}Ga -PSMA11 PET before starting clinical reporting is important so that physicians can provide appropriate reports regardless of what criteria are selected. Fendler et al. recommend initial training on at least 30 patient cases to ensure acceptable performance (8). Development of the EANM criteria was based on expert readers who had experience in reading more than 300 cases (9).

Intercriteria agreement ranged from substantial to almost perfect in our study. However, the definition of PSMA-RADS-3, including broad situations (4 subcategories) (11), can be often discordant with judgment based on the other criteria. There is a need to clearly state in the report which criteria were applied with the evidence of judgment. We also need to keep in mind that PSMA-ligand–negative PC can lead different judgments among the 3 criteria (Fig. 5).

One way the above-discussed challenges will be addressed is through the future use of artificial intelligence and machine learning to automate parts of image analysis and creation of reports. Recently, a growing number of successful results has been reported using machine learning for automatic organ segmentation, including prostate MRI (33–35). This technology has also been attempted in PSMA PET/CT for semiautomatic whole-body tumor burden assessment with a high yield of performance (36). As such, an artificial intelligence platform for clinical practice is expected to be developed and should aid with lesion identification and tracking over time.

Our retrospective study has some limitations. First, we could not confirm pathologic diagnoses in all lesions that were judged as positive. We focused on objectivity in evaluating ^{68}Ga -PSMA11 PET using the 3 criteria. Further studies are needed to assess the performance of each set of criteria in terms of diagnostic accuracy. Intercriteria agreement may have been overestimated because the readers interpreted images using the 3 criteria at the same time in each session. In addition, because the number of patients in each

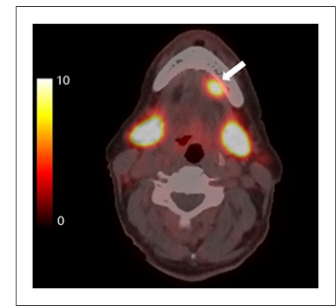


FIGURE 4. A 73-y-old man with BCR PC after high-dose external radiotherapy (prostate-specific antigen, 3.8 ng/mL). One reader pointed out asymmetric ^{68}Ga -PSMA11 uptake in left sublingual gland (arrow). Judgments were nonpathologic (other malignancy may be considered), equivocal (“consider positive” because of higher uptake than that of parotid glands), and PSMA-RADS-3C (intense uptake in site highly atypical of PC) based on EANM criteria, PROMISE, and PSMA-RADS, respectively. Further assessment of this uptake was not performed.

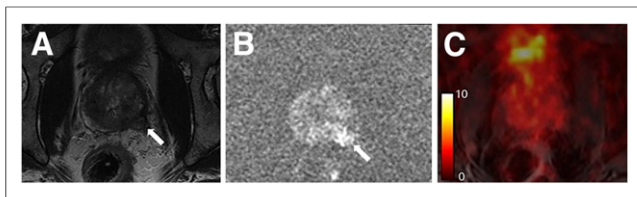


FIGURE 5. A 60-y-old man with biopsy-proven PC (prostate-specific antigen, 9.4 ng/mL; Gleason score, 4 + 5). (A and B) Primary tumor with invasion to left seminal vesicle (arrows) was clearly detected on T2-weighted (A) and diffusion-weighted (B) MR images. (C) However, this lesion did not have elevated ^{68}Ga -PSMA-11 uptake on fused PET/MR image. Although histopathologic evidence was unavailable, PSMA-ligand-negative PC was suspected. This primary tumor could be judged as negative (no uptake), positive (PI-RADS class 5), and equivocal (PSMA-RADS-3D) based on EANM criteria, PROMISE, and PSMA-RADS, respectively.

group (PET/MRI or PET/CT) was relatively small, further prospective studies enrolling larger populations are warranted.

CONCLUSION

The 3 proposed criteria (EANM, PROMISE, and PSMA-RADS) have good reproducibility in evaluating ^{68}Ga -PSMA11 PET. However, there are some factors causing interreader disagreement, indicating that further work is needed to harmonize or improve the criteria and find the right balance between accuracy and time requirements. This further work may include incorporation of machine learning or artificial intelligence in clinical workflows. Lastly, what works at one institution may not be well suited to another, leaving the door open for adoption of more than a single set of criteria.

DISCLOSURE

No potential conflict of interest relevant to this article was reported.

ACKNOWLEDGMENTS

We thank all the patients who participated and their families. We also thank our research coordinators, radiochemists, and technologists, as well as Tie Liang and Jarrett Rosenberg for assistance with statistical analyses.

KEY POINTS

QUESTION: Are there differences among the 3 different criteria (EANM, PROMISE, and PSMA-RADS) for interpretation of PSMA PET?

PERTINENT FINDINGS: In a retrospective review of data from 104 men with PC who had PSMA PET, nuclear medicine physicians independently evaluated at 2 different time points (6 mo apart) all images according to the 3 interpretation criteria. Overall, intrareader agreement was moderate to almost perfect. Intercriteria agreement for each site was moderate to almost perfect.

IMPLICATIONS FOR PATIENT CARE: Although the 3 published criteria have good intrareader reproducibility for reviewing PSMA PET, there are some factors causing interreader disagreement. Further work is needed to address this issue.

REFERENCES

1. Siegel RL, Miller KD, Jemal A. Cancer statistics, 2019. *CA Cancer J Clin*. 2019; 69:7–34.

- Ferlay J, Colombet M, Soerjomataram I, et al. Cancer incidence and mortality patterns in Europe: estimates for 40 countries and 25 major cancers in 2018. *Eur J Cancer*. 2018;103:356–387.
- Eiber M, Fendler WP, Rowe SP, et al. Prostate-specific membrane antigen ligands for imaging and therapy. *J Nucl Med*. 2017;58(suppl):67S–76S.
- Hicks RM, Simko JP, Westphalen AC, et al. Diagnostic accuracy of ^{68}Ga -PSMA-11 PET/MRI compared with multiparametric MRI in the detection of prostate cancer. *Radiology*. 2018;289:730–737.
- Park SY, Zacharias C, Harrison C, et al. Gallium 68 PMSA-11 PET/MR imaging in patients with intermediate- or high-risk prostate cancer. *Radiology*. 2018;288:495–505.
- Perera M, Papa N, Christidis D, et al. Sensitivity, specificity, and predictors of positive ^{68}Ga -prostate-specific membrane antigen positron emission tomography in advanced prostate cancer: a systematic review and meta-analysis. *Eur Urol*. 2016; 70:926–937.
- Eissa A, Elsherbiny A, Coelho RF, et al. The role of ^{68}Ga -PSMA PET/CT scan in biochemical recurrence after primary treatment for prostate cancer: a systematic review of the literature. *Minerva Urol Nefrol*. 2018;70:462–478.
- Fendler WP, Calais J, Allen-Auerbach M, et al. ^{68}Ga -PSMA-11 PET/CT inter-observer agreement for prostate cancer assessments: an international multicenter prospective study. *J Nucl Med*. 2017;58:1617–1623.
- Fanti S, Minozzi S, Morigi JJ, et al. Development of standardized image interpretation for ^{68}Ga -PSMA PET/CT to detect prostate cancer recurrent lesions. *Eur J Nucl Med Mol Imaging*. 2017;44:1622–1635.
- Eiber M, Herrmann K, Calais J, et al. Prostate cancer molecular imaging standardized evaluation (PROMISE): proposed mTNM classification for the interpretation of PSMA-ligand PET/CT. *J Nucl Med*. 2018;59:469–478.
- Rowe SP, Pienta KJ, Pomper MG, Gorin MA. Proposal for a structured reporting system for prostate-specific membrane antigen-targeted PET imaging: PSMA-RADS version 1.0. *J Nucl Med*. 2018;59:479–485.
- Eder M, Neels O, Muller M, et al. Novel preclinical and radiopharmaceutical aspects of [^{68}Ga]Ga-PSMA-HBED-CC: a new PET tracer for imaging of prostate cancer. *Pharmaceuticals (Basel)*. 2014;7:779–796.
- Weinreb JC, Barentsz JO, Choyke PL, et al. PI-RADS prostate imaging: reporting and data system—2015, version 2. *Eur Urol*. 2016;69:16–40.
- Gwet KL. Computing inter-rater reliability and its variance in the presence of high agreement. *Br J Math Stat Psychol*. 2008;61:29–48.
- Wongpakaran N, Wongpakaran T, Wedding D, Gwet KL. A comparison of Cohen's kappa and Gwet's AC1 when calculating inter-rater reliability coefficients: a study conducted with personality disorder samples. *BMC Med Res Methodol*. 2013;13:61.
- Gandaglia G, Abdollah F, Schifmann J, et al. Distribution of metastatic sites in patients with prostate cancer: a population-based analysis. *Prostate*. 2014;74: 210–216.
- Damjanovic J, Janssen JC, Furth C, et al. ^{68}Ga -PSMA-PET/CT for the evaluation of pulmonary metastases and opacities in patients with prostate cancer. *Cancer Imaging*. 2018;18:20.
- Li X, Rowe SP, Leal JP, et al. Semiquantitative parameters in PSMA-targeted PET imaging with ^{18}F -DCFPyL: variability in normal-organ uptake. *J Nucl Med*. 2017;58:942–946.
- Afshar-Oromieh A, Malcher A, Eder M, et al. PET imaging with a [^{68}Ga]gallium-labelled PSMA ligand for the diagnosis of prostate cancer: biodistribution in humans and first evaluation of tumour lesions. *Eur J Nucl Med Mol Imaging*. 2013;40:486–495.
- Sheikhabaei S, Afshar-Oromieh A, Eiber M, et al. Pearls and pitfalls in clinical interpretation of prostate-specific membrane antigen (PSMA)-targeted PET imaging. *Eur J Nucl Med Mol Imaging*. 2017;44:2117–2136.
- Fendler WP, Eiber M, Beheshti M, et al. ^{68}Ga -PSMA PET/CT: joint EANM and SNMMI procedure guideline for prostate cancer imaging: version 1.0. *Eur J Nucl Med Mol Imaging*. 2017;44:1014–1024.
- Freitag MT, Radtke JP, Afshar-Oromieh A, et al. Local recurrence of prostate cancer after radical prostatectomy is at risk to be missed in ^{68}Ga -PSMA-11-PET of PET/CT and PET/MRI: comparison with mpMRI integrated in simultaneous PET/MRI. *Eur J Nucl Med Mol Imaging*. 2017;44:776–787.
- Kabasakal L, Demirci E, Ocak M, et al. Evaluation of PSMA PET/CT imaging using a ^{68}Ga -HBED-CC ligand in patients with prostate cancer and the value of early pelvic imaging. *Nucl Med Commun*. 2015;36:582–587.
- Afshar-Oromieh A, Sattler LP, Mier W, et al. The clinical impact of additional late PET/CT imaging with ^{68}Ga -PSMA-11 (HBED-CC) in the diagnosis of prostate cancer. *J Nucl Med*. 2017;58:750–755.
- Will L, Giesel FL, Freitag MT, et al. Integration of CT urography improves diagnostic confidence of ^{68}Ga -PSMA-11 PET/CT in prostate cancer patients. *Cancer Imaging*. 2017;17:30.

26. Krohn T, Verburg FA, Pufe T, et al. [⁶⁸Ga]PSMA-HBED uptake mimicking lymph node metastasis in coeliac ganglia: an important pitfall in clinical practice. *Eur J Nucl Med Mol Imaging*. 2015;42:210–214.
27. Rischpler C, Beck TI, Okamoto S, et al. ⁶⁸Ga-PSMA-HBED-CC uptake in cervical, celiac, and sacral ganglia as an important pitfall in prostate cancer PET imaging. *J Nucl Med*. 2018;59:1406–1411.
28. Ahn T, Roberts MJ, Abduljabar A, et al. A review of prostate-specific membrane antigen (PSMA) positron emission tomography (PET) in renal cell carcinoma (RCC). *Mol Imaging Biol*. 2019;21:799–807.
29. Alipour R, Gupta S, Trethewey S. ⁶⁸Ga-PSMA uptake in combined hepatocellular cholangiocarcinoma with skeletal metastases. *Clin Nucl Med*. 2017;42:e452–e453.
30. Pyka T, Weirich G, Einspieler I, et al. ⁶⁸Ga-PSMA-HBED-CC PET for differential diagnosis of suggestive lung lesions in patients with prostate cancer. *J Nucl Med*. 2016;57:367–371.
31. Ferraro DA, Rupp NJ, Donati OF, Messerli M, Eberli D, Burger IA. ⁶⁸Ga-PSMA-11 PET/MR can be false positive in normal prostatic tissue. *Clin Nucl Med*. 2019;44:e291–e293.
32. Ardies PJ, Gykiere P, Goethals L, De Mey J, De Geeter F, Everaert H. PSMA uptake in mediastinal sarcoidosis. *Clin Nucl Med*. 2017;42:303–305.
33. Jia H, Xia Y, Song Y, et al. 3D APA-Net: 3D adversarial pyramid anisotropic convolutional network for prostate segmentation in MR images. *IEEE Trans Med Imaging*. July 11, 2019 [Epub ahead of print].
34. Tian Z, Liu L, Zhang Z, Xue J, Fei B. A supervoxel-based segmentation method for prostate MR images. *Med Phys*. 2017;44:558–569.
35. Cheng R, Lay N, Roth HR, et al. Fully automated prostate whole gland and central gland segmentation on MRI using holistically nested networks with short connections. *J Med Imaging (Bellingham)*. 2019;6:024007.
36. Gafita A, Bieth M, Kroenke M, et al. qPSMA: semiautomatic software for whole-body tumor burden assessment in prostate cancer using ⁶⁸Ga-PSMA11 PET/CT. *J Nucl Med*. 2019;60:1277–1283.